J|A|C|S COMMUNICATIONS

Published on Web 11/19/2009

Theoretical Predictions of Size-Dependent Carrier Mobility and Polarity in Graphene

Meng-Qiu Long,[†] Ling Tang,[†] Dong Wang,[†] Linjun Wang,[‡] and Zhigang Shuai*[,†,‡]

Department of Chemistry, Tsinghua University, Beijing 100084, P. R. China, and Key Laboratory of Organic Solids, Beijing National Laboratory for Molecular Sciences (BNLMS), Institute of Chemistry, Chinese Academy of Sciences, Beijing 100190, P. R. China

Received September 5, 2009; E-mail: zgshuai@tsinghua.edu.cn

Graphene nanoribbons (GNRs) have attracted intensive interest for nanoelectronics[1,2] because the charge mobility can reach as high as $2-25 \times 10^4$ cm^2 V^{-1} s^{-1} at room temperature (RT).[3−7] Even higher mobilities, up to 10^7 cm^2 V^{-1} s^{-1}, have been implied from magneto-absorption measurements on ultrapure graphene at low temperature.[8] Through first-principles calculations, we demonstrate that the RT mobility can reach 10^6 cm^2 V^{-1} s^{-1}. Most importantly, the polarity of the transport (i.e., whether it is electron or hole transport) can be tuned by nanoengineering of the graphene ribbon width. It is of primary interest to know how to cut a graphene sheet to achieve targeted transport properties.

Carrier mobility is the central issue for microelectronic semiconducting materials, especially in field-effect transistors.[9−11] To date, the scattering mechanism for carrier transport in graphene remains unclear.[12] Also, it is not clear how high the intrinsic carrier mobility for an ultrapure single-layered graphene sheet can be.[8] In an inorganic semiconductor such as Si, the electron coherence length is close to the acoustic phonon wavelength, which is much longer than the bond length; thus, the scattering of a thermal electron or hole arises mostly from the acoustic phonons, following the argument of Bardeen and Shockley.[13] We expect the situation to be similar in graphene because of the covalently bonded conjugated structure. The electron thermal energy is close to the acoustic phonon energy, and the deformation potential (DP) description is more appropriate to describe such a scattering process. It is assumed that the local deformations produced by a lattice wave are similar to the homogeneously deformed crystal. Under the effective mass approximation and the electron−acoustic phonon scattering mechanism, Bardeen and Shockley derived an analytical expression for the charge mobility (μ),[13] which can be recast for a one-dimensional DP[14] as

$$\mu = \frac{e\tau}{m^*} = \frac{e\hbar^2 C}{(2\pi k_B T)^{1/2}|m^*|^{3/2}E_1^{\,2}} \qquad (1)$$

in which τ is the acoustic phonon scattering relaxation time, $m^* = \hbar[\partial^2 E(k)/\partial k^2]^{-1}$ is the effective mass of the charge, and C is the stretching modulus caused by the longitudinal acoustic phonon along the ribbon, which is defined as $C = a_0[\partial^2 E(k_F)/\partial a^2]_{a=a_0}$, where $E(k)$ is the energy band and a and a_0 are the deformed and equilibrium lattice constants. In eq 1, E_1 is the DP constant, which is proportional to the stretching-induced band-edge shift $\delta E(k_F) = E_1(\delta a/a_0)$, where δa is a small change in the lattice constant that results in a position shift $\delta E(k_F)$ in the energy band near the Fermi surface. These quantities can be calculated using density functional theory (DFT) and have been previously applied in the study of functionalized carbon nanotubes.[15]

Optimized geometries and band structures of armchair GNRs (AGNRs) were computed using DFT in the generalized gradient approximation (GGA) with the Perdew−Burke−Ernzerhof (PBE) exchange correlation functional, as implemented in the Vienna ab initio simulation package (VASP).[16] The AGNR structure is shown in Figure 1. Hereafter, we represent the width of the ribbon by N, the number of carbon atoms along the side edge. The top and bottom edges were passivated by hydrogen.

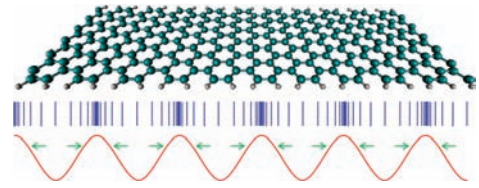

Figure 1. Schematic presentation of graphene and an acoustic phonon.

To calculate the DP constant E_1 and the stretching modulus C, additional band structures were calculated at lattice constants of $0.990a_0$, $0.995a_0$, $1.005a_0$, and $1.010a_0$ in order to perform finite differentiation to obtain both E_1 and C. All of the calculated results are shown in Table S1 in the Supporting Information for AGNRs with $N = 9-17$ for both electrons (conduction band) and holes (valence band); the relaxation times and mobilities were calculated according to eq 1 at RT.

Table S1 shows that all of the effective masses are in the range $0.057-0.077m_e$, which is close to the experimental value of $\sim 0.06m_e$ obtained by Novoselov et al.[1] No appreciable width dependence for the effective mass can be observed, and electrons and holes possess almost the same mass. The stretching modulus C increases steadily and slightly with the width of the AGNRs. This means that the rigidity of the AGNRs is enhanced with increasing nanoribbon width. The acoustic phonon scattering relaxation times were calculated to be in the range of a few tenths of a picosecond to a few tens of picoseconds, in good agreement with one recent experimental value of 20 ps.[8]

The most significant width dependence comes from the DP constant E_1, which is related to the longitudinal-deformation-induced band-edge shift, representing the scattering of an electron (conduction band edge) or hole (valence band edge) by the acoustic phonon. It is noted that for $N = 3k$ (i.e., $N = 9, 12, 15$), E_1 for holes is $\sim$1 order of magnitude larger than that for electrons, while for $N = 3k + 1$ or $3k + 2$, E_1 for electrons is $\sim$1 order of magnitude larger than that for holes. This results in a difference of 2 orders of magnitude in the mobilities of electrons and holes by virtue of eq 1. The calculated width-dependent charge mobilities for both polarities are displayed in Figure 2. To illustrate the DP effect, which characterizes the electron or hole coupling with the acoustic phonon, we have also plotted the band-edge shifts with respect to the lattice constant variations in Figure S3 in the Supporting Information. It is seen that the fit is perfectly linear, with the slope being the DP constant E_1.

[†] Tsinghua University.
[‡] Beijing National Laboratory for Molecular Sciences.

10.1021/ja907528a

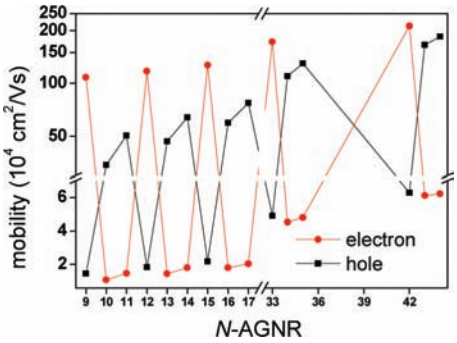

Figure 2. Theoretically predicted mobility dependence on the width of graphene for both polarities.

It is thus intriguing to understand such staggeringly oscillating behavior. To do this, we turned to the wave functions of the band-edge state at the Γ point, which are equivalent to the frontier molecular orbitals [i.e., the highest occupied molecular orbital (HOMO) for the hole and the lowest unoccupied molecular orbital (LUMO) for the electron] responsible for transport. These are shown in Figure 3 for $N = 12$ and 13 (the $N = 14$ case is not shown because it is exactly the same as for $N = 13$). The red dashed line stands for the longitudinal direction of the ribbon axes (i.e., the direction of stretching). For $N = 12$ ($3k$), it is noted that the bonding direction for the HOMO is vertical, while for the LUMO, the bonding character is horizontally connected. Thus, the HOMO is vertically localized perpendicular to the stretching direction, while the LUMO is delocalized along the stretching axis. The band-edge shift due to ribbon stretching comes from the site energy instead of the hopping integral (or bandwidth). It is thus expected that the localized HOMO (hole state) is scattered more strongly by the acoustic phonon than the LUMO (electron state) for $N = 3k$. Similarly, for $N = 13$ (or 14), the hole is scattered much more strongly than the electron by the acoustic phonon (see Figure 3).

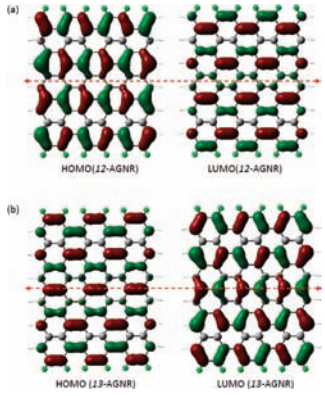

Figure 3. Γ-point HOMO and LUMO wave functions for AGNRs with (a) $N = 12$ and (b) $N = 13$. The red dashed line stands for the direction of stretching.

We next examined the zigzag GNR (ZGNR), which is a more stable form. The conduction and valence bands merge flatly near the Fermi surface (see Figure S2). The effective mass approximation is not applicable. We thus directly applied the Boltzmann transport equation method without invoking the effective mass approximation, which is more general.[16] There is no size-dependent carrier polarity, and the mobility is ∼2 orders of magnitude lower than that of the AGNR (see Figure 4). This is due to the flat band near the Fermi surface, which means the "effective mass" is much larger. Under the situation of doping, the band goes to the more dispersed part, and the mobility increases.

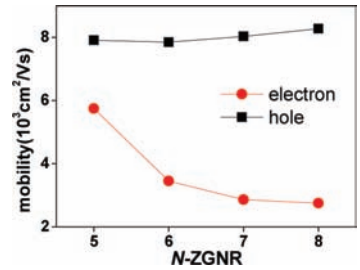

Figure 4. Calculated mobilities for the ZGNR as a function of width N.

To conclude, we have calculated the charge mobility of graphene using first-principles methods. We have found that the width of the ribbon plays an important role in the tuning the polarity of carrier transport in AGNRs, which exhibits a distinct $3k$ alternating behavior: for $N = 3$k, the intrinsic electron RT mobility can reach $>10^6$ cm^2 V^{-1} s^{-1}, and the hole mobility is ∼2 orders of magnitude less; for $N = 3k + 1$ or $3k + 2$, the hole mobility is calculated to be $4-8 \times 10^5$ cm^2 V^{-1} s^{-1} and the electron mobility $\sim 10^4$ cm^2 V^{-1} s^{-1}. No alternating size dependence was found for ZGNRs. By exfoliation, it is difficult to control width, but chemists now can control the width through synthesis. It will thus be intriguing to combine chemists' controlled structure with physicists' nanoelectronics to reveal the size effect predicted in this work.

Acknowledgment. This work was supported by the Ministry of Science and Technology of China (Grants 2006CB806200, 2006CB0N0100, and 2009CB623600) and the National Natural Science Foundation of China.

Supporting Information Available: One-dimensional DP theory, band structures, computational details and results (Table S1), and band-edge shifts. This material is available free of charge via the Internet at http://pubs.acs.org.

References

(1) Novoselov, K. S.; Geim, A. K.; Morozov, S. V.; Jiang, D.; Zhang, Y.; Dubonos, S. V.; Grigorieva, I. V.; Firsov, A. A. *Science* **2004**, *306*, 666. Bunch, J. S.; van der Zande, A. M.; Verbridge, S. S.; Frank, I. W.; Tanenbaum, D. M.; Parpia, J. M.; Craighead, H. G.; McEuen, P. L. *Science* **2007**, *315*, 490. Han, M. Y.; Özyilmaz, B.; Zhang, Y.; Kim, P. *Phys. Rev. Lett.* **2007**, *98*, 206805.
(2) Chen, F.; Qing, Q.; Xia, J. L.; Li, J. H.; Tao, N. J. *J. Am. Chem. Soc.* **2009**, *131*, 9908. Areshkin, D. A.; Gunlycke, D.; White, C. T. *Nano Lett.* **2007**, *7*, 204.
(3) Berger, C.; Song, Z.; Li, X.; Wu, X.; Brown, N.; Naud, C.; Mayou, D.; Li, T.; Hass, J.; Marchenkov, A. N.; Conrad, E. H.; First, P. N.; de Heer, W. A. *Science* **2006**, *312*, 1191.
(4) Tan, Y.-W.; Zhang, Y.; Bolotin, K.; Zhao, Y.; Adam, S.; Hwang, E. H.; Sarma, S. D.; Stormer, H. L.; Kim, P. *Phys. Rev. Lett.* **2007**, *99*, 246803.
(5) Du, X.; Skachko, I.; Barker, A.; Andrei, E. Y. *Nat. Nanotechnol.* **2008**, *3*, 491.
(6) Bolotin, K. I.; Sikes, K. J.; Jiang, Z.; Fundenberg, G.; Hone, J.; Kim, P.; Stormer, H. L. *Solid State Commun.* **2008**, *146*, 351.
(7) Orlita, M.; Faugeras, C.; Plochocka, P.; Neugebauer, P.; Martinez, G.; Maude, D. K.; Barra, A.-L.; Sprinkle, M.; Berger, C.; de Heer, W. A.; Potemskil, M. *Phys. Rev. Lett.* **2008**, *101*, 267601.
(8) Neugebauer, P.; Ortila, M.; Faugeras, C.; Bara, A.-L.; Potemski, M. *Phys. Rev. Lett.* **2009**, *103*, 136403.
(9) Lin, Y.-M.; Jenkins, K. A.; Valdes-Garcia, A.; Small, J. P.; Farmer, D. B.; Avouris, P. *Nano Lett.* **2009**, *9*, 422.
(10) Ang, P. K.; Chen, W.; Wee, A. T. S.; Loh, K. P. *J. Am. Chem. Soc.* **2008**, *130*, 14392.
(11) Luo, Z. T.; Lu, Y.; Somers, L. A.; Johnson, A. T. C. *J. Am. Chem. Soc.* **2009**, *131*, 898.
(12) Tian, F.; Konar, A.; Xing, H. L.; Jena, D. *Phys. Rev. B* **2008**, *78*, 205403.
(13) Bardeen, J.; Shockley, W. *Phys. Rev.* **1950**, *80*, 72.
(14) Beleznay, F. B.; Bogar, F.; Ladik, J. *J. Chem. Phys.* **2003**, *119*, 5690.
(15) Sa, N.; Wang, G.; Yin, B.; Huang, Y. *Physica E* **2008**, *40*, 2396.
(16) Tang, L.; Long, M.; Wang, D.; Shuai, Z. *Sci. China, Ser. B: Chem.* **2009**, *52*, 1519.

JA907528A